Si en moyenne les déplacements mesurés et calculés sont du même ordre de grandeur, par contre les valeurs relatives du désordre des atomes de métal et de carbone sont inversées. Cela est sans doute lié au fait que la proportion de défauts dans $ThC_{0,77}$ est trop élevée pour que leur interaction puisse être négligée; il faudrait de plus tenir compte dans le calcul de la variation des constantes de forces avec la composition.

Enfin, il est intéressant de mentionner les résultats d'expériences similaires par diffraction de neutrons – étude de spectres complets – par Karimov, Ern, Chidrov & Faïzoullaiev (1977), ou de rayons X – étude d'une seule raie de diffraction – par Timofeeva & Klochkov (1974), à 300 K sur des carbures de métaux de transition. En particulier, les valeurs des amplitudes de déplacements statiques moyennées sur les deux types d'atomes données par ces auteurs pour le composé $ZrC_{0,8}$ sont respectivement 2 et 1,4%, valeurs légèrement supérieures au désordre trouvé dans $ThC_{0,77}$.

Les auteurs tiennent à adresser leurs remerciements à P. Wolfers pour son programme d'intégration des raies de diffraction de neutrons et à L. Zuppiroli pour ses conseils lors de l'ajustement des courbes. Nous remercions particulièrement D. Lesueur pour ses commentaires judicieux.

References

BACON, G. E. (1962). *Neutron Diffraction*. Oxford University Press.

CHIPMAN, D. R. & PASKIN, A. (1959). *J. Appl. Phys.* **30**, 1992–2002.

COCHRAN, W. & KARTHA, G. (1956). *Acta Cryst.* **9**, 941–943.

DANAN, J. (1975). *J. Nucl. Mater.* **57**, 280–282.

FELDMAN, J. L. (1975). *Phys. Rev. B*, **12**, 813–814.

HEWAT, A. W. (1972). *J. Phys. C*, **5**, 1309–1316.

ILL (1977). *Neutron Beam Facilities at the HFR Available for Users*, pp. 17–25.

KARIMOV, I., ERN, V. T., CHIDROV, I. & FAÏZOULLAIEV, F. (1977). *Fiz. Met. Metalloved.* **44**, 184–186.

KRIVOGLAZ, M. A. (1969). *Theory of X-ray and Thermal Neutron Scattering by Real Crystals*, pp. 220–248. New York: Plenum Press.

LESUEUR, D. (1976). Non publié.

MAURICE, V., BOUTARD, J. L. & ABBÉ, D. (1979). *J. Phys.* **40**, C4, 140–141.

NOVION, C. H. DE (1976). *Plutonium and Other Actinides*, edité par H. BLANCK & R. LINDNER, pp. 877–891. Amsterdam: North-Holland.

NOVION, C. H. DE, FENDER, B. E. F. & JUST, W. (1976). *Plutonium and Other Actinides*, edité par H. BLANCK & R. LINDNER, pp. 893–901. Amsterdam: North-Holland.

PADEL, A. (1970). *Rapp. CEA*, R 3953, p. 36.

SUORTTI, P. (1967). *Ann. Acad. Sci. Fenn. Ser. A*6, n° 240.

TIMOFEEVA, I. & KLOCHKOV, L. A. (1974). *Refractory Carbides*, edité par G. V. SAMSONOV, pp. 239–246. New York et London: Consultants Bureau.

TOTH, L. E. (1971). *Transition Metal Carbides and Nitrides*. New York et London: Academic Press.

WEDGWOOD, F. A. (1974). *J. Phys. C*, **7**, 3203–3218.

WEDGWOOD, F. A. & DE NOVION, C. H. (1974). Non publié.

WILLIS, B. T. M. (1970). *Acta Cryst.* A**26**, 396–401.

Acta Cryst. (1980). A**36**, 921–929

Paracrystals and Growth-Disorder Models

BY T. R. WELBERRY, G. H. MILLER AND C. E. CARROLL

Research School of Chemistry, Australian National University, PO Box 4, Canberra, ACT 2600, Australia

(*Received* 24 *September* 1979; *accepted* 16 *May* 1980)

Abstract

Some problems of the paracrystal model of diffraction from distorted lattices are discussed. The relationship between paracrystals and crystal growth-disorder models is established and the latter are used to generate examples of distorted lattices having many of the properties envisaged for paracrystals without some of the drawbacks.

1. Introduction

The concept of the 'paracrystal' was introduced by Hosemann and co-workers and extensively developed by them over a number of years prior to the publication of a book (Hosemann & Bagchi, 1962) containing a summary of the work. Since that time the paracrystal model has been widely used as a theoretical model for describing the diffraction properties of distorted lattices. Because of its success in describing observed diffraction effects qualitatively or even semi-quantitatively the mathematical basis of the model went unquestioned for many years until Perrett & Ruland (1971) discovered that the 'ideal paracrystal' model predicted density fluctuations dependent on the size of the crystal, contrary to experimental experience with high polymers. This inadequacy has been removed in practice by use of the so-called α^* law (Hosemann,

0567-7394/80/060921-09$01.00

1975), which limits the size of paracrystalline grains so that fluctuations never get too large. Nevertheless, Brämer (1975) and Brämer & Ruland (1976) have further criticized the mathematical basis of the model.

The most popular form of the model is the 'ideal paracrystal'. This is constructed from two intersecting one-dimensional ($1D$) chains of lattice points, each chain being a $1D$ paracrystal in which successive vectors vary in length and direction independently of previous vectors. The two-dimensional ($2D$) model is then constructed by completing parallelograms from primary vectors in the two chains. This model has the advantage that the diffraction properties are easily calculated but has the disadvantage that the variance of the length of vectors between successively distant neighbours increases without bound. As a result the model gives an unsatisfactory description of small-angle scattering properties. More general models of paracrystals described by Hosemann & Bagchi (1962), while perhaps being more realistic than the 'ideal paracrystal', do not allow simple calculation of their diffraction properties and moreover are not easily constructed.

The paracrystal model is clearly an example of models of spatially interacting random variables and as such was developed at a time when little was known in this very difficult and complex field. While many advances have been made in this area in recent years with the work of Bartlett (1967), Besag (1974), Dobrushin (1968), Moussouri (1974), Spitzer (1971), Whittle (1954) and others it remains imperfectly understood and few explicit results are available still. Because of this, any model which is reasonably tractable is of interest even though it may have properties different from the most general models. One such model has been studied extensively in recent years by the present authors. This is a model involving only binary variables which has been used to describe the way in which substitutional disorder may be introduced into crystals at growth (Welberry & Galbraith, 1973; Welberry, 1977; Miller & Welberry, 1979). While this growth-disorder model does not represent the most general form for disordered binary lattices it has yielded a number of explicit solutions, is easily simulated and moreover still allows a considerable diversity of the statistical properties of the lattice.

We have been struck for some time by the similarity of the way in which growth-disorder models are constructed and the methods used by Hosemann and co-workers for attempting to produce realizations of general paracrystals. In this paper we explore this relationship by extending the binary growth-disorder models to ones using continuous variables. We thus show how lattice realizations may be produced which have properties similar to those for the original paracrystal concept but which do not suffer from some of its drawbacks.

Within the sections that follow we give examples of optical diffraction patterns of lattice realizations which were produced in the manner described by Harburn, Miller & Welberry (1974) using an Optronics P-1700 photomation system. The diffraction patterns were recorded using a laser diffractometer similar to that described in Harburn, Taylor & Welberry (1975). In constructing the lattice realizations, Gaussian-distributed random numbers were generated using the IBM scientific subroutine *GAUSS* in conjunction with a generator of uniformly distributed pseudo-random numbers. This latter involved a procedure in which a table of one hundred random numbers was used to ensure satisfactory independence. A call to the subroutine *RANDU* was used to select a number from the table and a second call to replace it with a newly generated one.

2. Paracrystals and perturbed regular lattices

The formulation of paracrystals by Hosemann and co-workers was in terms of fluctuating vectors which represented the unit-cell edges. The 'ideal paracrystal' is a case for which solutions are available because in $3D$ the lattices consist of three independent $1D$ chains, the $3D$ lattice being formed by completing parallelepipeds from the primary vectors. Guinier (1963) doubted the validity of the 'ideal paracrystalline model' since it seemed unreasonable to expect independent fluctuations of interatomic vectors in $3D$. Hammersley (1967) in discussing 'harnesses' goes even further by saying that it is unreasonable to assign independent random variables to the edges of an n-dimensional lattice ($n \geq 2$) since there are many more cell edges than lattice points. Because of this, severe conditional dependency conditions must be imposed on the vector distributions, and it seems more reasonable to work with variables representing the lattice points than with the vectors between points. This view appears to have been taken unanimously by the mathematical probabilists working in this field who were mentioned in the *Introduction*. In $1D$, with lattice points and cell edges being equal in number, the two approaches are equally tenable and in this section we compare the two by considering a simple example.

(i) *Paracrystal*

Suppose we have a simple $1D$ paracrystal in which the only variability is in the length, d, of the primitive vector. Suppose also that the lengths of vectors are independently but identically and normally distributed,

$$P(d) = K \exp\left[-\frac{(d-a_0)^2}{2\sigma_p^2}\right], \qquad (1)$$

where a_0 is the mean cell length and σ_p the standard deviation. K is a normalizing constant which will be used in subsequent equations with the same meaning

but not necessarily the same value. The distribution of the combined length of n such successive independent vectors is given by

$$P_n(d) = K \exp\left[-\frac{(d - na_0)^2}{2n\sigma_p^2}\right]. \quad (2)$$

Equation (2) shows the linear increase of the variance with n which is typical of $1D$ paracrystals. It will be noted that (2) is derived from (1) by assuming independence of successive vectors and thus is a special case of a more general model in which the length of one vector is correlated with the length of neighbouring vectors. However, since specification of the joint probability of two neighbouring vectors including correlation would involve the positions of three lattice points, we shall not consider this for comparison with models specified in terms of only nearest-neighbour lattice points.

(ii) *Perturbed regular lattice*

We consider a regular $1D$ lattice of spacing a_0 and consider random perturbations x_i about each site where the x_i are longitudinal displacements. Thus the spacing d_i between the $(i-1)$th and ith points is $x_i - x_{i-1} + a_0$. We consider a simple model in which all x_i are identically normally distributed and the joint distribution of two neighbouring variables is also normal. That is,

$$P(x_i) = K \exp\left[-\frac{x_i^2}{2\sigma_L^2}\right] \quad (3)$$

$$P(x_{i-1}, x_i) = K \exp\left[-\frac{1}{2\sigma_L^2} \cdot \frac{(x_{i-1}^2 + x_i^2 - 2rx_{i-1}x_i)}{(1 - r^2)}\right], \quad (4)$$

where σ_L is the standard deviation of the displacements from the underlying regular lattice points, and r is a correlation coefficient,

$$r = \frac{\langle x_{i-1} x_i \rangle}{\sigma_L^2}.$$

Given (3) and (4), the conditional probability of x_i given x_{i-1} can be determined as

$$P(x_i/x_{i-1}) = \frac{P(x_{i-1}, x_i)}{P(x_i)} = K \exp\left[-\frac{1}{2\sigma_L^2} \frac{(x_i - rx_{i-1})^2}{(1 - r^2)}\right]. \quad (5)$$

A realization of the model is produced by using (3) to generate the first point and then (5) for successive points. The lattice produced will be immediately stationary with properties (3) and (4). For comparison with the paracrystal model we require the distribution of $d_i = (x_i - x_{i-1} + a_0)$. This is readily shown to be

$$P(d_i) = K \exp\left[-\frac{1}{2\sigma_L^2} \cdot \frac{(d_i - a_0)^2}{2(1 - r)}\right]. \quad (6)$$

A property of the model defined by (3) and (5), which is in fact a simple Markov chain, is that the correlation coefficients between successively distant variables go as r^n; so (6) can be generalized for comparison with (2) as

$$P_n(d) = P(x_i - x_{i-n} + na_0) = K \exp\left[-\frac{1}{2\sigma_L^2} \cdot \frac{(d - na_0)^2}{2(1 - r^n)}\right]. \quad (7)$$

From (7) we see that for the case of a perturbed regular lattice the variance increases with n as the effect of the correlation diminishes but reaches a bounded value of twice the nearest-neighbour variance.

(iii) *Comparison of the diffraction properties*

The intensity of diffraction is obtained by Fourier transformation of the autocorrelation function. This in both cases is

$$A(d) = \sum_n P_n(d). \quad (8)$$

In the Appendix we derive the intensity of diffraction for a $1D$ perturbed regular lattice. It is instructive to compare the two models for cases where the nearest-neighbour distributions (1) and (6) are identical, that is, when

$$\sigma_p^2 = \sigma_L^2\, 2(1 - r). \quad (9)$$

In Fig. 1 we plot the first 11 terms of the autocorrelation function for a value of $\sigma_p = 0{\cdot}1789a_0$. In

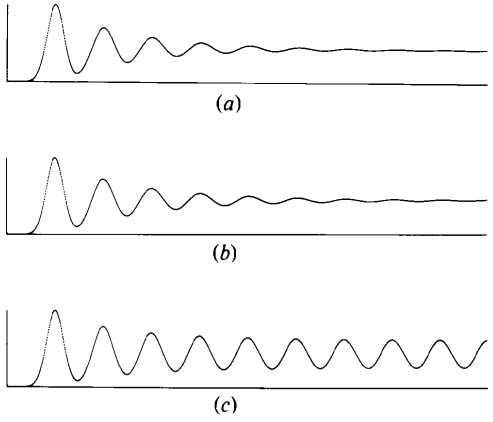

Fig. 1. Plots of the first 11 terms of the autocorrelation function $A(d)$ given by (*a*) equation (2) for the paracrystal and (*b*) and (*c*) equation (7) for the perturbed regular lattice. In all three the distribution of the lengths of nearest-neighbour vectors is the same.

Fig. 1(*a*) we use (2) for the paracrystal; for 1(*b*) we use (7) with $\sigma_L = 0{\cdot}6a_0$ and $r = 0{\cdot}9555$; and for 1(*c*) we use (7) with $\sigma_L = 0{\cdot}2a_0$ and $r = 0{\cdot}6$. It will be seen that while Fig. 1(*c*) is distinctly different from 1(*a*), Fig. 1(*b*) is remarkably similar to 1(*a*). With σ_L as low as $0{\cdot}2a_0$ the underlying regular lattice is easily discernible by the residual ripple in $A(d)$ but with $\sigma_L = 0{\cdot}6a_0$ the underlying lattice is virtually undetectable.

In Fig. 2 we show optical diffraction patterns of simulations of these three models. In the diffraction masks from which they were produced, each $1D$ chain consisted of only 512 points and to produce a reasonably noise-free diffraction pattern many such chains were placed on each mask with arbitrary positions so that the *intensity* from each should be added to give the total diffracted intensity. It is seen that while Figs. 2(*a*) and (*b*) are very similar, the sharp first-order lattice peak due to the underlying regular lattice is clearly still visible in Fig. 2(*c*).

For any given nearest-neighbour distribution it is always possible to choose σ_L large enough that the underlying lattice is undetectable and correspondingly increase r to maintain the constancy of $\sigma_L\, 2(1-r)$ in

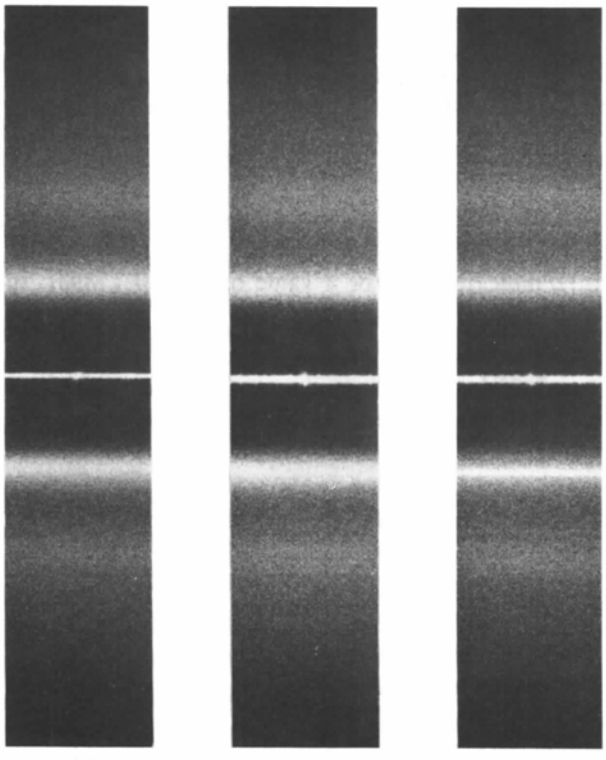

(*a*) (*b*) (*c*)

Fig. 2. Optical diffraction patterns of the $1D$ lattices whose auto-correlation functions are shown in Fig. 1. Note the similarity of (*a*) and (*b*) and the sharp first-order maximum within the diffuse peak in (*c*).

(9). We can rewrite the exponent denominator in (7) using the binomial expansion

$$2\sigma_L^2\, 2(1-r^n) = 4\sigma_L^2\, n(1-r)\left[1 - \frac{(n-1)}{2!}(1-r) + \frac{(n-1)(n-2)}{3!}(1-r)^2 - \text{higher terms}\right].$$

Neglecting all but the first term in the expansion, we may rewrite equation (7) as

$$P_n(d) = K \exp\left[-\frac{1}{2\sigma_L^2}\frac{(d-na_0)^2}{2n(1-r)}\right]. \qquad (10)$$

It will be noticed that as r approaches unity for any fixed n the neglected terms go to zero so that in this limit the general pair distribution functions (2) and (7) become equal. The neglected terms vanish when $n = 1$. But when r is fixed they are significant when n is sufficiently large; for such values of n, $P_n(d)$ may or may not contribute significantly to the diffraction patterns.

To obtain further information on small values of $1 - r$, we consider how successive cell vectors are correlated in the perturbed regular lattice. Suppose $d_i = x_i - x_{i-1}$. We wish to find a correlation coefficient

$$R = \frac{\langle d_i\, d_{i-1}\rangle}{\langle d_i^2\rangle}.$$

Expanding d's in terms of x's, we find

$$\langle d_i\, d_{i-1}\rangle = \langle x_i\, x_{i-1}\rangle + \langle x_{i-1}\, x_{i-2}\rangle - \langle x_i\, x_{i-2}\rangle - \langle x_{i-1}\rangle^2 = -\sigma_L^2(1-r)^2$$

and $\langle d_i^2\rangle = 2\sigma_L^2(1-r)$,

hence $$R = -\tfrac{1}{2}(1-r). \qquad (11)$$

Thus as r approaches unity the correlation coefficient between the lengths of neighbouring vectors approaches zero. For the example of Figs. 1(*b*) and 2(*b*) $R = -0{\cdot}0222$ while for the example of Figs. 1(*c*) and 2(*c*) $R = -0{\cdot}2$. In the second case the model is considerably different from a paracrystal.

Although we have made no attempt to make the above arguments completely rigorous we have demonstrated that the two models, the first using a description in terms of variable cell edges and the second in terms of variable lattice positions, are equivalent in the limit as r approaches unity while $\sigma_L^2 \times 2(1-r)$ remains constant. However, while the paracrystal approach gives a variance that increases with n beyond all bounds, the perturbed regular lattice

approach gives a variance that is bounded *except* in the limit of $r = 1$. For $r < 1$ the negative correlation R in (11) between successive cell vectors provides the necessary restraint on the displacements to keep them within finite bounds.

3. Gaussian growth-disorder models

Growth-disorder models are stochastic models involving binary variables in more than $1D$ which have been developed to describe the way in which disorder can be introduced into crystals at growth, the two values of the variables representing either two different molecular or atomic species or two different orientations of the same species. Among other things the models enable actual realizations of disordered lattices to be produced very rapidly by means of a simple algorithm. It has been shown, however, that they are only special cases of more general Ising models which in fact represent the most general form of nearest-neighbour lattice models for binary variables, but these cannot be simulated directly (but indirectly as they occur as equilibrium distributions in certain spatial–temporal processes) and very few explicit results are available for them. Despite the fact that growth-disorder models give rise to only special cases of more general distributions they do still allow considerable variation of statistical properties to be built into a lattice, and, because of this and the extreme ease with which realizations can be produced, they continue to be of interest in their own right.

The most general binary model based on interactions within the generic unit cell $ABCD$ (see Fig. 3) is an Ising model defined as follows. The probability that the lattice has a particular configuration c is

$$P_c = \frac{1}{Z} \exp[-E_c/kT],$$

where Z is the partition function or normalizing factor and E_c is the interaction energy (Hamiltonian).

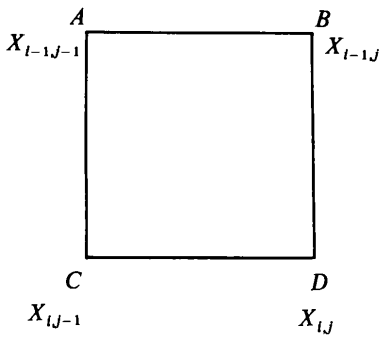

Fig. 3. The spatial arrangement of the variables.

$$E_c = \sum_{\substack{\text{all}\\ \text{sites}}} x_{i,j}(H + J_1 x_{i-1,j} + J_2 x_{i,j-1} + J_3 x_{i-1,j-1} + J_4 x_{i-1,j+1} + K_1 x_{i-1,j} x_{i,j-1} + K_2 x_{i-1,j-1} x_{i-1,j} + K_3 x_{i-1,j-1} x_{i,j-1} + K_4 x_{i-1,j} x_{i-1,j+1} + L x_{i,j-1} x_{i-1,j-1} x_{i-1,j}), \tag{12}$$

where $x_{i,j}$ are binary variables which may take values ± 1, and H, J, K, L are the energies associated with one-, two-, three- and four-body interactions respectively.

Given this definition, which is an example of a Gibbs ensemble, we are interested in the marginal distribution on the generic unit cell $ABCD$, *i.e.* the joint probability $P(x_A, x_B, x_C, x_D)$. The problem is quite intractable in the general case because of the difficulties in determining Z. However, a growth-disorder model subset of this Ising model exists in which the distribution $P(x_A, x_B, x_C, x_D)$ is factorizable in a way that can be utilized. We may always write

$$P(x_A, x_B, x_C, x_D) = P(x_A)\, P(x_B/x_A)\, P(x_C/x_A, x_B)\, P(x_D/x_A, x_B, x_C), \tag{13}$$

but by imposing the condition

$$P(x_C/x_A, x_B) \equiv P(x_C/x_A), \tag{14}$$

(13) takes the form

$$P(x_A, x_B, x_C, x_D) = P(x_A)\, P(x_B/x_A)\, P(x_C/x_A)\, P(x_D/x_A, x_B, x_C). \tag{15}$$

With the factorization (15) realizations may be constructed using $P(x_A)$ for the first point, $P(x_B/x_A)$ and $P(x_C/x_A)$ for boundary edges and $P(x_D/x_A, x_B, x_C)$ for all other general points. The product form of (15) implies that each of these probabilities can be used independently. An attempt to construct a lattice using (13) would fail because a point being added has simultaneously to satisfy, for example, $P(x_C/x_A, x_B)$ and $P(x_D/x_A, x_B, x_C)$ in different cells. The lattice distribution obtained by using the factorization (15) will be immediately stationary with marginal distributions $P(x_A)$ for single points, $P(x_A, x_B) = P(x_A)\, P(x_B/x_A)$ and $P(x_A, x_C) = P(x_A)\, P(x_C/x_A)$ for pairs of points and $P(x_A, x_B, x_C, x_D)$ for cells formed by four points. For further details and proofs see Pickard (1978), Welberry, Miller & Pickard (1979) and Pickard (1979).

Equation (14) represents the minimum constraint necessary on $P(x_A, x_B, x_C, x_D)$ for the model to be constructed in growth-disorder model fashion. However, we shall concern ourselves only with cases

for which $P(x_A, x_B, x_C, x_D)$ is also symmetric to reflection in either vertical or horizontal planes. Examples of realizations of this symmetric model are to be found in Welberry (1977).

We can develop continuous variable models along exactly the same lines as (12)–(15) if $x_{i,j}$ is taken to be a continuous rather than a discrete variable, although (12) now does not represent the most general form for the interaction Hamiltonian. In order to use continuous variables we need to find a probability distribution $P(x_A, x_B, x_C, x_D)$ which suitably factorizes as (15). A type of continuous random variable commonly used in the literature is the Gaussian variable and we shall proceed using these.

The most general form having rectangular symmetry, for a Gaussian distribution of four variables, is

$$\begin{aligned} P(x_A, x_B, x_C, x_D) = K \exp - \{[&x_A^2 + x_B^2 + x_C^2 + x_D^2 \\ &- 2r'(x_A x_B + x_C x_D) \\ &- 2s'(x_A x_C + x_B x_D) \\ &- 2t'(x_A x_D + x_B x_C)]/C\}, \end{aligned} \quad (16)$$

where r', s', t', C are simple functions of r, s and t, the horizontal, vertical and diagonal correlation coefficients.

We find that in order to factorize this in the form of (15) we need to impose $t = rs$, *i.e.* the diagonal correlation coefficient is the product of the two axial correlation coefficients. This is exactly the same condition on the correlation coefficients as occurs for the binary variable models. Given this restriction the various factors of (15) become

$$P(x_A) = K \exp - \left\{ \frac{x_A^2}{2\sigma^2} \right\} \quad (17)$$

$$P(x_B/x_A) = K \exp - \left\{ \frac{(x_B - rx_A)^2}{2\sigma^2(1-r^2)} \right\} \quad (18)$$

$$P(x_C/x_A) = K \exp - \left\{ \frac{(x_C - sx_A)^2}{2\sigma^2(1-s^2)} \right\} \quad (19)$$

$$P(x_D/x_A, x_B, x_C) = K \exp - \left\{ \frac{(x_D - sx_B - rx_C + rsx_A)^2}{2\sigma^2(1-r^2)(1-s^2)} \right\} \quad (20)$$

$$\begin{aligned} P(x_A, x_B, x_C, x_D) = K \exp - \{[&x_A^2 + x_B^2 + x_C^2 + x_D^2 \\ &- 2r(x_A x_B + x_C x_D) \\ &- 2s(x_A x_C + x_B x_D) \\ &+ 2rs(x_A x_D + x_B x_C)] \\ &\times [2\sigma^2(1-r^2)(1-s^2)]^{-1}\}. \end{aligned} \quad (21)$$

Here σ is the standard deviation of the single site variable and K as before is a normalizing constant which has a different value in each equation. Just as for the binary model this Gaussian model has Markov chains embedded along every pathway in the lattice whose steps along each of the axes are always in the same direction. Because of this the correlation field has the simple form

$$\rho_{mn} = r^{|m|} s^{|n|}.$$

We now consider the use of this model for the production of paracrystal-like lattices. We can use exactly the same arguments as for the $1D$ case outlined in § 2 and all of the results derived there apply equally here. Additionally, we need to consider displacements in both x and y directions. Each may have different correlation fields and values of σ. For simplicity, in the examples that follow the x and y displacements have the same value of σ and are mutually independent.

Fig. 4 illustrates the effect of varying both the standard devation, σ, and the correlation coefficients, r and s, which in this case have the same value ρ. Fig. 4(a) shows optical diffraction patterns for lattices having $\sigma = 0{\cdot}5a_0$ and $\rho = 0{\cdot}95$ and $0{\cdot}99$. Note that the correlation coefficient, R, between the lengths of neighbouring vectors is $-0{\cdot}025$ and $-0{\cdot}005$ for these two respectively. Fig. 4(b) shows patterns for lattices having $\sigma = a_0$ and the same value of ρ as in Fig. 4(a). Fig. 5 shows small representative portions of the diffraction masks from which the patterns in Fig. 4 were produced.

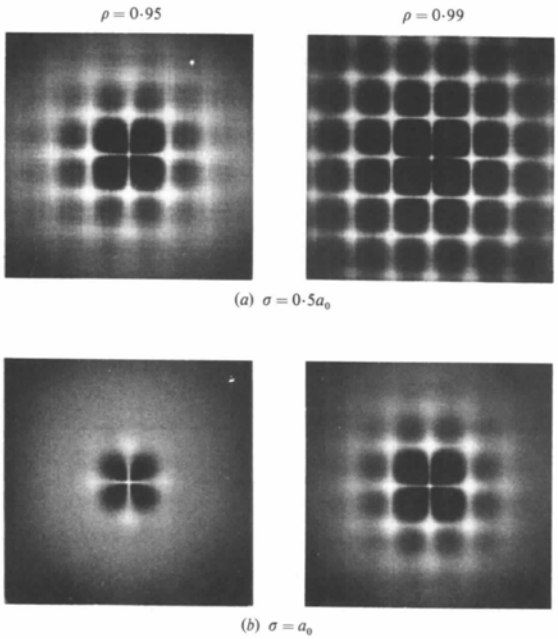

Fig. 4. Optical diffraction patterns of Gaussian variable growth-disorder models. ρ is the correlation coefficient between the displacements of lattice points which are nearest neighbours, in both the x and y directions, and it applies independently to displacements in both the x and y directions. σ is the standard deviation of the displacement of lattice points from the underlying regular lattice of spacing a_0.

Fig. 6 illustrates the effect of having different correlation fields for the two displacements. The correlation coefficient for displacements transverse to the direction of correlation is ρ_T and for displacements in the direction of correlation the correlation coefficient is ρ_L. Thus for example in Fig. 6(*a*) the correlation coefficient for x displacements is 0·99 in the x direction and 0·95 in the y direction and for y displacements the correlation values are reversed. That is, in this case, the longitudinal correlations are stronger than the transverse ones. In Fig. 6(*b*) the transverse correlations are stronger than the longitudinal ones. Fig. 7 shows small representative portions of the diffraction masks from which the patterns in Fig. 6 were produced.

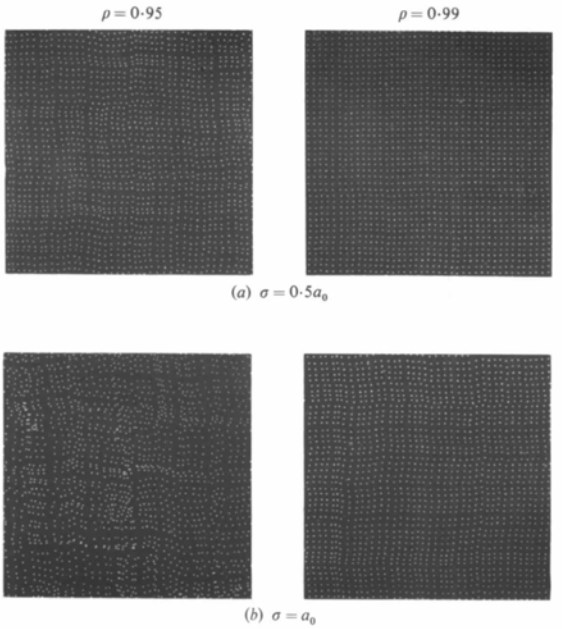

Fig. 5. Small representative portions of the optical diffraction masks used to obtain the diffraction patterns of Fig. 4. The originals contained 512 × 512 points.

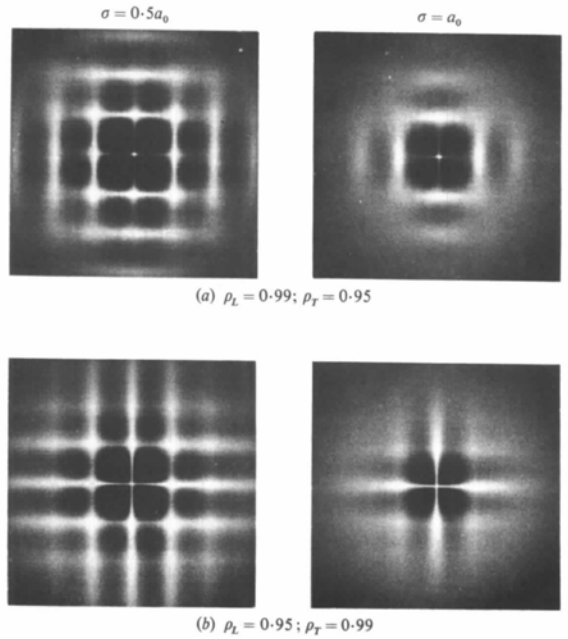

Fig. 6. Optical diffraction patterns of Gaussian variable growth-disorder models. ρ_T and ρ_L are transverse and longitudinal correlation coefficients between displacements of nearest-neighbour lattice points (see text). σ is the standard deviation of the displacement of lattice points from the underlying regular lattice of spacing a_0.

4. Generalizations

It is interesting to conjecture on the results of allowing the growth-disorder model formulation to be generalized. The restriction on the form of $P(x_A, x_B, x_C, x_D)$ given in (16) was necessary in order for the distribution to be produced in a growth-disorder model fashion. This could have been left in a more general form in which the correlations between points adjacent in the [11] and [1$\bar{1}$] directions were more (or less) dominant. A model with this as the basic cell distribution would give diffraction patterns in which the (1,1) and (1,$\bar{1}$) maxima were more (or less) dominant than in the examples in Figs. 4 and 6. The only way in which such distributions could be produced would be by an iterative procedure similar to that by which realizations of the Ising model may be produced.

A further generalization could be in the form of the interaction energy E_c of (12). The possibilities are so

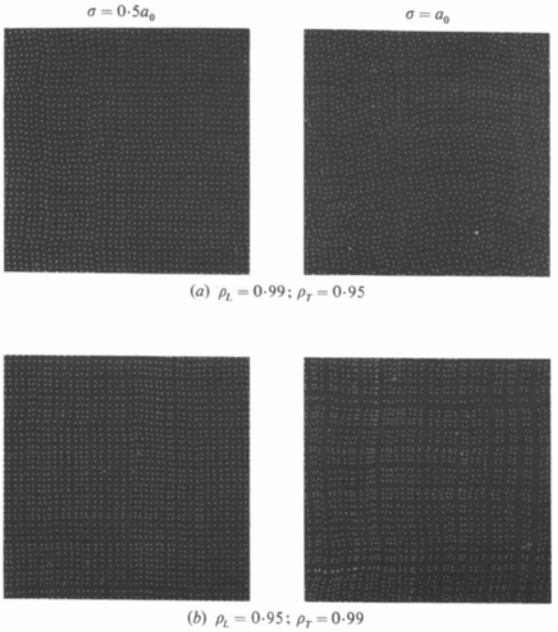

Fig. 7. Small representative portions of the optical diffraction masks used to obtain the diffraction patterns of Fig. 6. The originals contained 512 × 512 points.

numerous that any conjecture seems not to be worthwhile. Brook (1964) gives an example of a model formulated in a rather different joint probability way but involving only nearest-neighbour interactions. When this is re-expressed in terms of the type of conditional probabilities used in growth-disorder models it is seen to involve relationships with more distant neighbours. It may be that extensions along these lines would be fruitful, but realizations would again be produced only with great difficulty.

The Gaussian variables used are not the only ones to which the treatment given in § 3 could be applied, but the functional forms for the conditional probabilities (18)–(20) would certainly be less convenient and it is doubtful whether any significantly different results would be obtained.

The general methods described in § 3 work equally well in three (or more) dimensions.

5. Conclusion

We have demonstrated that lattices having diffraction properties very similar to paracrystals may be quite readily generated using a model related to crystal growth-disorder models. The main difference in their properties is that the variance of the length of vectors of successively more distant neighbours is bounded for our lattices which means that the underlying regular lattice is always detectable in principle if not in practice. However, the work of Hammersley (1967) on harnesses suggests strongly that in $3D$ the very fact that points are indexable necessarily constrains them to lie within a finite distance of the correspondingly indexed points of an underlying regular lattice. If this is the case it seems unreasonable to expect the $3D$ analogue of the unbounded $1D$ paracrystal to exist. Our model approaches the 'ideal paracrystal' model as the correlation values tend to unity.

APPENDIX

We derive the diffraction pattern of a $1D$ perturbed regular lattice defined by equations (3) and (4) in the text.

Suppose for simplicity that the lattice constant a_0 is unity so that the nth point is at a position $z_n = n + x_n$ and the mth point at $z_m = m + x_m$ where x_n, x_m are random values of the displacement. The scattered intensity is

$$\left|\sum_n \exp[ik(n + x_n)]\right|^2 = \sum_n \exp[ik(n + x_n)] \sum_m \exp[-ik(m + x_m)].$$

The ensemble average of this is proportional to

$$\sum_l \exp(ikl)\,\langle \exp[ik(x_m - x_n)]\rangle$$

where $l = m - n$.

The correlation coefficient between x_m and x_n is $S = r^{|l|}$ and x_m and x_n are identically distributed as in (3). Thus

$$\langle \exp[ik(x_m - x_n)]\rangle = K \int\int \exp[ik(x_m - x_n)] \times \exp\left[\frac{x_m^2 + x_n^2}{2\sigma^2(1 - S^2)} + \frac{S x_m x_n}{\sigma^2(1 - S^2)}\right] dx_n\, dx_m$$

$$= \exp|-(1 - S)(k\sigma)|$$

and the diffracted intensity becomes

$$I(k) = \sum_l \exp(ikl)\,\exp[-(1 - r^{|l|})(k\sigma)^2]$$

$$I(k) = \exp(-k^2\sigma^2) \sum_l \exp(\sigma^2 k^2 r^{|l|}) \exp(ikl).$$

If $|r| < 1$ this can be split into two parts,

$$I(k)_{\text{Bragg}} = \exp(-k^2\sigma^2) \sum_l \exp(ikl)$$

and

$$I(k)_{\text{diffuse}} = \exp(-k^2\sigma^2) \times \sum_{l=-\infty}^{\infty} [\exp(\sigma^2 k^2 r^{|l|}) - 1] \exp(ikl)$$

$$= \exp(-k^2\sigma^2) \sum_{P=1}^{\infty} \frac{(k^2\sigma^2)^P}{P!} \sum_{l=-\infty}^{\infty} r^{P|l|} \exp(ikl)$$

$$= \exp(-k^2\sigma^2) \times \sum_{P=1}^{\infty} \frac{(k^2\sigma^2)^P}{P!} \frac{1 - r^{2P}}{1 + r^{2P} - 2r^P \cos(k)}.$$

The Bragg intensity consists of peaks of magnitude $\exp(-k^2\sigma^2)$ at positions for which k is a multiple of 2π. For σ equal to unity (*i.e.* the same as the cell spacing) the intensity of the first-order Bragg peak relative to the origin peak is $7 \times 10^{-18} : 1$, while for $\sigma = 0{\cdot}5$ the ratio is $5 \times 10^{-5} : 1$. It is thus virtually undetectable for these values of σ.

For very small values of σ for which $k^4\sigma^4$ is negligible, terms in the diffuse intensity with $P > 1$ may

be neglected and the familiar formula for short-range-order diffuse scattering (see *e.g.* Guinier, 1963, p. 269) is obtained. For values of σ much greater than this many such diffuse curves corresponding to higher values of P must be included in the summation. Each of these will represent successively broader more diffuse peaks as r^{2P} approaches zero. The factor $(k^2\sigma^2)^P/P!$ eventually goes to zero as P increases for any σ but for values of $\sigma \simeq 1$ many terms must be included.

References

BARTLETT, M. S. (1967). *J. R. Stat. Soc. A*, **130**, 467–477.
BESAG, J. (1974). *J. R. Stat. Soc. B*, **36**, 192–225.
BRÄMER, R. (1975). *Acta Cryst.* A**31**, 551–560.
BRÄMER, R. & RULAND, W. (1976). *Makromol. Chem.* **177**, 3601–3617.
BROOK, D. (1964). *Biometrika*, **51**, 481–483.
DOBRUSHIN, R. L. (1968). *Theory Probab. Its Appl. (USSR)*, **13**, 197–224.
GUINIER, A. (1963). *X-ray Diffraction*. San Francisco: Freeman.
HAMMERSLEY, J. M. (1967). *Proceedings of the Fifth Berkeley Symposium on Mathematical Statistics and Probability*, **3**, 89–118.
HARBURN, G., MILLER, J. S. & WELBERRY, T. R. (1974). *J. Appl. Cryst.* **7**, 36–38.
HARBURN, G., TAYLOR, C. A. & WELBERRY, T. R. (1975). *Atlas of Optical Transformations*. London: Bell.
HOSEMANN, R. (1975). *J. Polym. Sci.* **50**, 265–281.
HOSEMANN, R. & BAGCHI, S. N. (1962). *Direct Analysis of Diffraction by Matter*. Amsterdam: North Holland.
MILLER, G. H. & WELBERRY, T. R. (1979). *Acta Cryst.* A**35**, 391–400.
MOUSSOURI, J. (1974). *J. Stat. Phys.* **10**, 11–33.
PERRET, R. & RULAND, W. (1971). *Kolloid Z. Z. Polym.* **247**, 835–843.
PICKARD, D. K. (1978). *Suppl. Adv. Appl. Probab.* **10**, 58–64.
PICKARD, D. K. (1979). In the press.
SPITZER, F. (1971). *Am. Math. Mon.* **78**, 142–154.
WELBERRY, T. R. (1977). *Proc. R. Soc. London Ser. A*, **353**, 363–376.
WELBERRY, T. R. & GALBRAITH, R. F. (1973). *J. Appl. Cryst.* **6**, 87–96.
WELBERRY, T. R., MILLER, G. H. & PICKARD, D. K. (1979). *Proc. R. Soc. London Ser. A*, **367**, 175–192.
WHITTLE, P. (1954). *Biometrika*, **41**, 434–449.

Acta Cryst. (1980). A**36**, 929–936

Relationship between 'Observed' and 'True' Intensity: Effect of Various Counting Modes

BY A. J. C. WILSON

Department of Physics, University of Birmingham, Birmingham B15 2TT, England

(*Received* 1 *June* 1978; *accepted* 27 *June* 1980)

Abstract

Expressions for the probability $p(R_o)$ that a reflexion of 'true' intensity R will have an observed value R_o (possibly negative) are obtained for four counting modes: fixed-time counting, equal and unequal times for total and background; fixed-count timing, equal and unequal counts for total and background. The distributions have a positive excess and are in general skew, though the skewness may be zero for particular choices of unequal times (counts). Deviations from the normal distribution with the same mean and variance may be considerable for $|R_o| \simeq 0$ and for $|R_o|$ large, and may possibly be significant in some applications even for $R_o \simeq R$. This apparent conflict with the central limit theorem is reconciled.

0567-7394/80/060929-08$01.00

1. Introduction

In both single-crystal and powder diffractometry the integrated intensity of a reflexion is obtained as the difference between a counting rate averaged over a region of reciprocal space intended to include the reflected intensity, and a counting rate averaged over a neighbouring volume of reciprocal space intended to include only background. If the intentions are not effectively realized there will be a systematic error in the measured intensity, but the present concern is not with such systematic errors but with statistical fluctuations in the intensity as observed. Although an intensity can never be really negative, it is not uncommon for the measured background counting rate to be higher than the measured reflexion-plus-background rate, giving an